

Short communication

Z. GATZIOUFAS^{1,2}, F. HAFEZI¹, K. KOPSIDAS², S. THANOS²

DYSFUNCTIONAL UVEOSCLERAL PATHWAY IN A RAT MODEL OF CONGENITAL GLAUCOMA

¹Department of Ophthalmology, University Hospitals of Geneva HUG, Geneva, Switzerland;

²Institute of Experimental Ophthalmology, University of Muenster, Muenster, Germany

The purpose of the study was to investigate the presence of the uveoscleral pathway in the normotensive rat (NR) and in a rat model of congenital glaucoma (CGR). We injected the fluorescent tracer 70-kDa dextran rhodamine B in the anterior chamber of four NRs and four CGRs. At 10 and 60 minutes after injection, rats were euthanized by CO₂ inhalation and eyes were enucleated. Cryosections were prepared and analyzed using fluorescent microscopy. Hematoxylin-eosin staining and electron microscopy of the anterior chamber angle (ACA) were performed. At 10 minutes after injection, fluorescent tracer was detected in the iris root and ciliary processes of NRs and CGRs. At 60 minutes, NRs showed prominent signal in the suprachoroidal, whereas, in the CGRs, tracer was barely detectable. Histology of the anterior chamber revealed the presence of an open ACA and electron microscopy confirmed the normal structure of the ciliary body in CGRs. Conclusions: Our results document the presence of an uveoscleral pathway in the normotensive rat. The rat model of congenital glaucoma shows severe impairment of the uveoscleral pathway, suggesting that alterations of the uveoscleral outflow might play a role in the pathogenesis of CG.

Key words: *congenital glaucoma, uveoscleral pathway, optic nerve, ciliary body, intraocular pressure*

INTRODUCTION

Aqueous humor drainage from the anterior chamber predominantly consists of two routes: the conventional trabecular meshwork pathway and the uveoscleral outflow pathway (1). The uveoscleral pathway is a drainage route for aqueous humor from the anterior chamber that successively includes extracellular spaces within the iris root, the ciliary muscle, the anterior choroid and suprachoroidal space, and the adjacent sclera. Experimental studies demonstrated the presence of an uveoscleral pathway as a secondary drainage mechanism for aqueous humor in humans, monkeys, rabbits, dogs, pigs and mice (1-4). Published data suggest that it accounts for less than 15% of the total outflow in humans, but it varies considerably in other mammals; it represents 40–60% of the total outflow facility in monkeys, whereas it is significantly less in cats and rabbits (3–8%) (5).

We investigate the presence of an uveoscleral pathway in the normotensive rat (NR) as well as in a rat model of congenital glaucoma (CGR). The glaucoma rat strain used in our experiments is characterized by prominent buphthalmos and middle-wide anterior chamber with open irido-corneal angle, as well as by atrophied optic nerve head, resembling human inherited buphthalmos (6, 7). The colony has been established as a regular breeding strain over 8 years and retinal ganglion cell pathology as well as proteomic analysis of the glaucomatous damage occurring in this model is well documented (8, 9).

MATERIALS AND METHODS

Intraocular pressure (IOP) was measured under topical anesthesia. One drop of proparacaine 0.5% was administered in each eye before IOP measurement (URSA-Pharm, Saarbrucken, Germany). All measurements were performed in a single session between 9:00 a.m. and 12:00 p.m. with the aid of Tono-Pen XL (Reichert Technologies, NY, USA). At least 10 IOP readings were recorded and averaged for each eye.

All rats were anesthetized by a peritoneal injection of a mixture of ketamine-sulfate (40 mg/kg) and xylazine (10 mg/kg). Under an operation microscope, with the aid of a glass micropipette, 2 µL of 0.2 pg/µL of the fluorescent tracer 70-kDa dextran rhodamine B (Invitrogen, OR, USA) were injected in the anterior chamber of the left rat eye in four NRs as well as in four CGRs. Prior to the dextran rhodamine B injection, a similar quantity of aqueous humor was aspirated from the anterior chamber. Postoperatively, gentamycin ointment was applied once. After survival times of 10 and 60 minutes the rats were euthanized by CO₂ inhalation. Eyes were enucleated, cryosections (12 µm) were prepared and analysed using fluorescent microscopy. Sixteen cryosections from the NRs (four from each rat) and sixteen cryosections from the CGRs (four from each rat) were processed with the Axiovision version 4.8.1 software program (Carl Zeiss, Jena, Germany) and further analyzed for quantification of the fluorescence intensity using the free-share ImageJ software program (NIH, Bethesda, Maryland, USA). Statistical analysis was performed by an experienced

independent investigator with the aid of SPSS software program version 17.0, using the Mann-Whitney test. P values below 0.05 were considered statistically significant. Data are represented as mean \pm standard error of the mean in arbitrary units (AU).

Paraffin sections were stained with haematoxylin and eosin and examined by light microscopy for comparison. All procedures were performed in accordance with the ARVO guidelines on the use of animals in research.

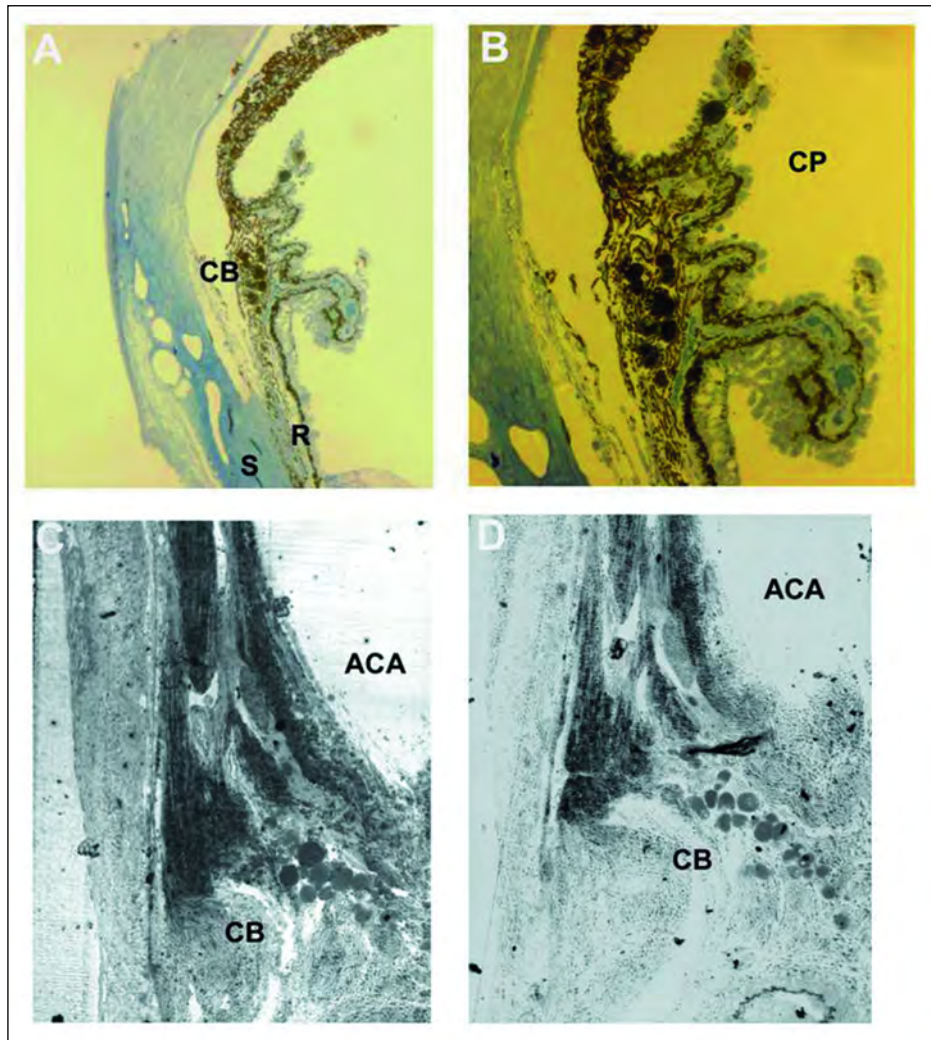


Fig. 1. Haematoxylin-eosin staining. Anatomy of the ciliary body and suprachoroidal space in the rat with congenital glaucoma. Histology reveals the presence of an open, middle-wide anterior chamber angle (*Fig. 1A, 1B*). The ciliary body appears to have a normal structure in electron microscopy (*Fig. 1C, 1D*). CB: ciliary body; S: sclera; R: retina; ACA: anterior chamber angle.

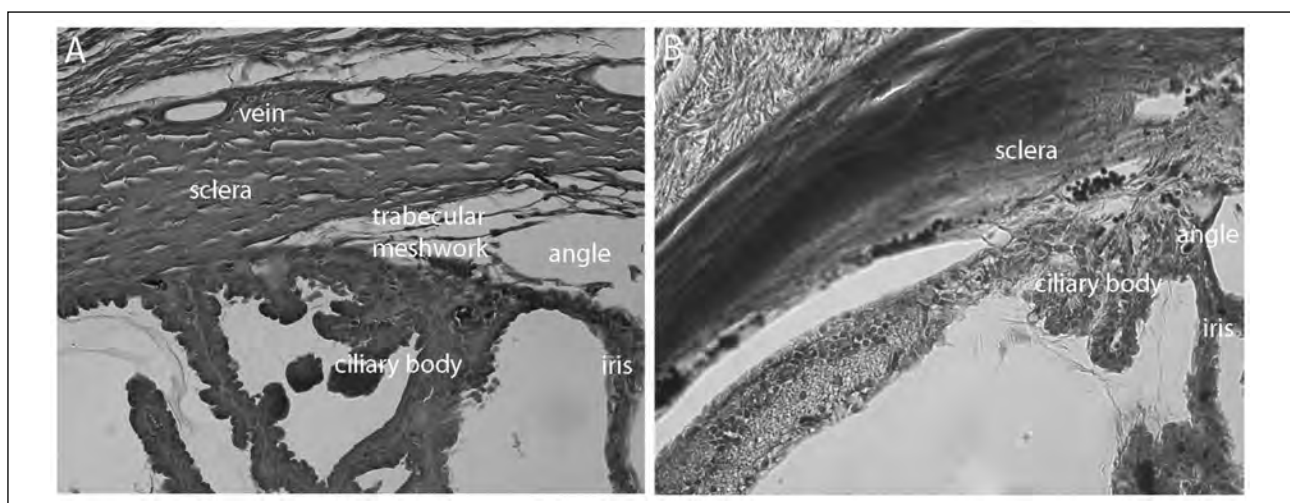


Fig. 2. Anatomy of the anterior chamber angle in the normal rat (*A*) and in the rat with congenital glaucoma (*B*). The normal rat demonstrated a well-structured trabecular meshwork, which was not the case in the rat with congenital glaucoma.

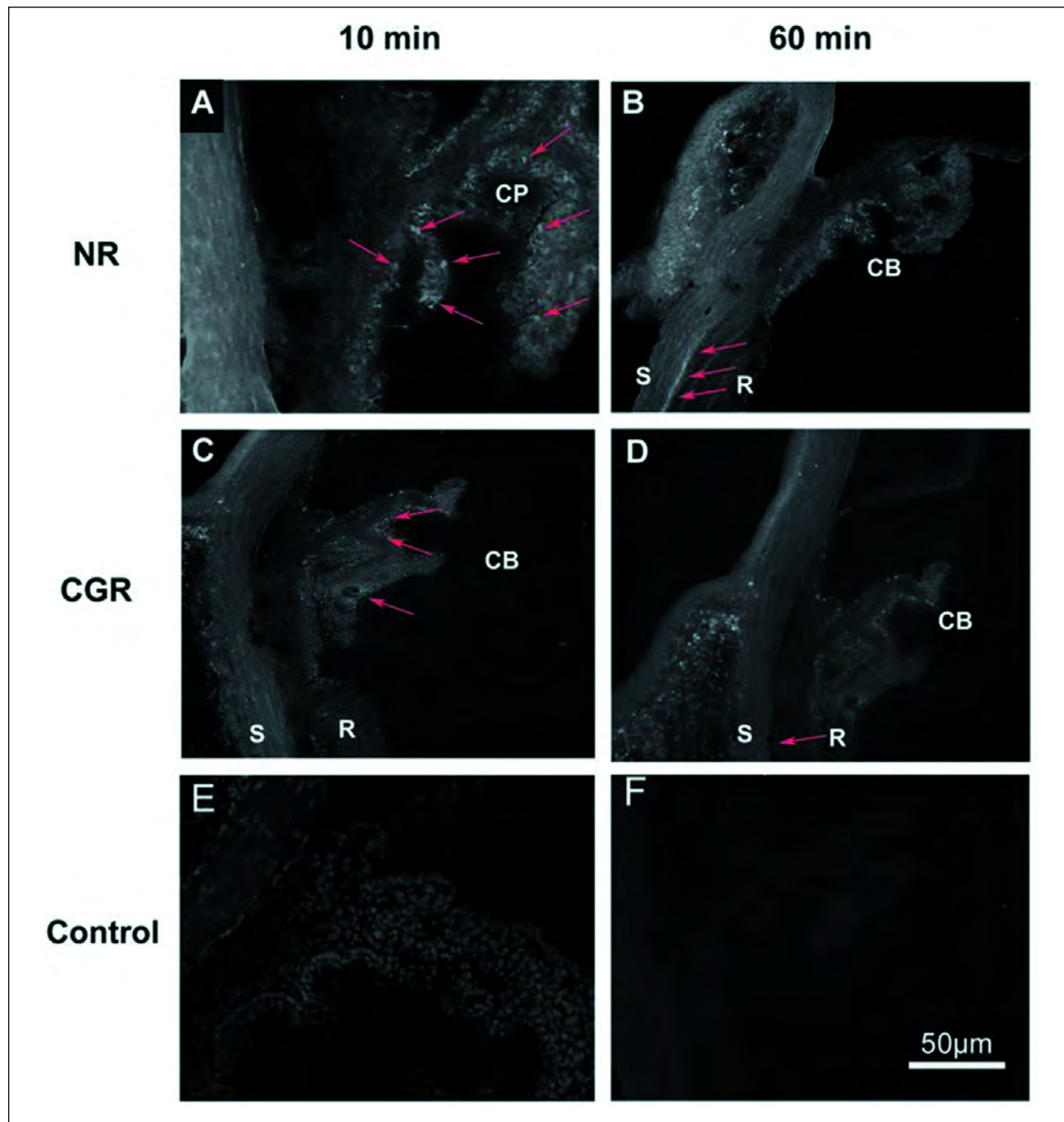


Fig. 3. Fluorescent microscopy of the ciliary body and suprachoroidal space after fluorescent dextran injection in the anterior chamber of normotensive rats and rats with congenital glaucoma. The red arrows indicate the fluorescent signal due to dextran. Ten minutes after the fluorescent tracer injection we detected a prominent fluorescent signal in the iris root and the iris ciliary processes of the NR group (*Fig. 3A*), whereas the fluorescent staining in the CGR group had similar distribution but the signal intensity was reduced (*Fig. 3C*). Sixty minutes after the fluorescent tracer injection we detected an intense signal between the choroid and sclera of the NR group (*Fig. 3B*), while fluorescent staining in the suprachoroidal space of the CGR group was almost absent (*Fig. 3D*).

NR: normotensive rats; CGR: rats with congenital glaucoma; CB: ciliary body; CP: ciliary processes; S: sclera; R: retina

RESULTS

Four 1.5-year-old animals were used for experiments in each group. The IOP was 14.6 ± 2.2 mm Hg in the NR group and 34.4 ± 6.1 mm Hg in the CGR group. Corneal diameter was 6.7 ± 0.1 mm in the NR group and 10.2 ± 1.4 mm in the CGR group.

The anterior chamber angle (ACA) in the rat eye is well described and displays great structural and functional similarities to the corresponding area of the human eye (10). The structure of ciliary body and the suprachoroidal space in the rat model of congenital glaucoma was depicted in paraffin eye sections stained with haematoxylin and eosin (*Fig. 1*). Histology revealed the presence of an open, middle-wide anterior chamber

angle (*Fig. 1A, 1B*). However, the NR group demonstrated a well-structured trabecular meshwork, which was not the case in the CGR group (*Fig. 2*).

The ciliary body showed a regular micro-structure in electron microscopy (*Fig. 1C, 1D*). All glaucomatous eyes showed similar findings.

Fluorescent microscopy of eye sections prepared 10 minutes after the fluorescent tracer injection revealed a prominent fluorescent signal in the iris root and the iris ciliary processes of the NR group (*Fig. 3A*), whereas the fluorescent staining in the CGR group had similar distribution, but the signal intensity was reduced (*Fig. 3C*). Examination by fluorescent microscopy of sections prepared 60 minutes after the fluorescent tracer injection revealed an intense signal between the choroid and sclera of the NR group (*Fig. 3B*), while fluorescent staining in the suprachoroidal space of the CGR group was almost absent (*Fig. 3D*). The fluorescent signal in iris root and ciliary processes was significantly reduced. Fluorescence was not observed in the anterior segment of the contralateral eye in both groups.

Semi-quantitative analysis of the fluorescence intensity revealed a mean intensity of 2.8 ± 0.4 for the NRs, whereas the mean intensity for the CGRs was 0.6 ± 0.3 ($p < 0.001$). There were no statistically significant differences in fluorescence intensity between the NRs or between the CGRs.

DISCUSSION

Uveoscleral pathway is a secondary aqueous humor drainage route, which has been well established in humans, monkey, mouse and many other mammals by use of fluorescent dextran as a marker for the aqueous humor dynamic flow. Histological studies have revealed that no epithelial barrier exists between the anterior chamber and the supraciliary space (11). For this reason alone, it is concluded that the rate at which substances pass from the anterior chamber into the supraciliary space depends on the permeability of the ciliary muscle (11). The contribution of the uveoscleral pathway to the total aqueous humor outflow as well as the rate of uveoscleral drainage is varying significantly among different species (11). However, there is only limited evidence regarding the physiology of uveoscleral pathway in the rat (12, 13).

Several diverse tracers have been used in different species to delineate the uveoscleral outflow pathway. Fluorescent dextrans are extremely stable *in vivo* and *in vitro*, characterized by only minimal tissue binding properties and therefore suitable as markers for the functional documentation of the aqueous humor outflow (14, 15).

In the present study, following a 70-kDa dextran rhodamine B injection in the anterior chamber of NRs and CGRs, fluorescent was observed after 10 minutes in the iris root and ciliary processes of both groups, although signal intensity was decreased in the CGR group. Fluorescent staining in the suprachoroidal space was detectable at 60 minutes after the initial injection only in the NR group. The fluorescent signal in the CGR group was almost absent. The absence of fluorescence in the iris root and ciliary processes after 60 minutes in both groups indicates that tissue binding of the dextran was minimal and the progression of the fluorescent tracer reflects indeed the aqueous humor drainage from the anterior chamber.

Anatomy of the ACA did not appear to differ significantly in CGRs when compared to NRs, as examined by hematoxylin-eosin staining. However, the trabecular meshwork in the iridocorneal angle was not well-structured. The fact that anatomical integrity of the trabecular meshwork was not preserved in the CGR group, which is in agreement with the

findings of Tawara and Inomata, who documented that developmental immaturity of the trabecular meshwork may be one the primary causes of increased intraocular pressure in congenital glaucoma (16). Electron microscopy revealed the presence of normal micro-structure of the ciliary body in CGRs.

Our study did not reveal any anatomical changes that may account for the functional impairment of the uveoscleral pathway in the CGR group. However, based on the fact that subcanalicular accumulation of extracellular matrix is one of the main causes of congenital glaucoma (17), we assume that potential deposition of abnormal tissue in the suprachoroidal space may contribute to the dysfunction of the uveoscleral pathway. However, this hypothesis requires further investigation. Moreover, preliminary data demonstrate potential impairment of the optic tract input to the intergeniculate leaflet of the thalamus, which is normally mediated by glutamate acting *via* non-NMDA ionotropic receptors (18) and it is associated with the visuomotor and sleep/arousal systems (19).

The results of our study document the presence of the uveoscleral pathway in the normal rat and reveal an impairment of this drainage route in our rodent model of CG. It seems that dysfunction of the uveoscleral pathway might play an additional role in the pathogenesis of CG and therefore further investigation of the uveoscleral mechanism in CG would be of paramount importance.

Financial support: None.

Conflict of interest: None declared.

REFERENCES

- Bill A. Conventional and uveoscleral drainage of aqueous humor in the cynomolgus monkey (*Macaca irus*) at normal and high intraocular pressures. *Exp Eye Res* 1966; 5: 45-54.
- McMaster PR, Macri FJ. Secondary aqueous humor outflow pathways in the rabbit, cat and monkey. *Arch Ophthalmol* 1968; 79: 297-303.
- Krohn J, Bertelsen T. Corrosion casts of the suprachoroidal space and uveoscleral drainage routes in the pig eye. *Acta Ophthalmol Scand* 1997; 75: 28-31.
- Lindsey JD, Weinreb RN. Identification of the mouse uveoscleral outflow pathway using fluorescent dextran. *Invest Ophthalmol Vis Sci* 2002; 43: 2201-2205.
- Nilsson SF. The uveoscleral outflow routes. *Eye (Lond)* 1997; 11: 149-154.
- Thanos S, Naskar R. Correlation between retinal ganglion cell death and chronically developing inherited glaucoma in a new rat mutant. *Exp Eye Res* 2004; 79: 119-129.
- Naskar R, Thanos S. Retinal gene profiling in a hereditary rodent model of elevated intraocular pressure. *Mol Vis* 2006; 12: 1199-1210.
- Lasseck J, Schroer U, Koenig S, Thanos S. Regeneration of retinal ganglion cell axons in organ culture is increased in rats with hereditary buphthalmos. *Exp Eye Res* 2007; 85: 90-104.
- Gatziofias Z, Charalambous P, Seitz B, et al. Cholinergic inhibition by botulinum toxin in a rat model of congenital glaucoma raises intraocular pressure. *Br J Ophthalmol* 2008; 92: 826-831.
- Van der Zypen E. Experimental morphological study on structure and function of the filtration angle of the rat eye. *Ophthalmologica* 1977; 174: 285-298.
- Pederson JE. Uveoscleral outflow. In: The Glaucomas, Ritch R, Shields MB, Krupin T, (eds). St. Louis, Mosby, 1996: pp. 337-343.

12. Lindsey JD, Hofer A, Wright KN, Weinreb RN. Partitioning of the aqueous outflow in rat eyes. *Invest Ophthalmol Vis Sci* 2009; 50: 5754-5758.
13. Camelo S, Shanley A, Voon AS, McMenamin PG. The distribution of antigen in lymphoid tissues following its injection into the anterior chamber of the rat eye. *J Immunol* 2004; 172: 5388-5395.
14. Schroder U, Arfors KE, Tangen O. Stability of fluorescein labelled dextrans in vivo and in vitro. *Microvasc Res* 1976; 11: 33-39.
15. Toris CB, Gregerson DS, Pederson JE. Uveoscleral outflow using different-sized fluorescent tracers in normal and inflamed eyes. *Exp Eye Res* 1987; 45: 525-532.
16. Tawara A, Inomata H. Developmental immaturity of the trabecular meshwork in congenital glaucoma. *Am J Ophthalmol* 1981; 92: 508-525.
17. Ueno A, Tawara A, Kubota T, Ohnishi Y, Inomata H, Solomon AS. Histopathological changes in iridocorneal angle of inherited glaucoma in rabbits. *Graefe's Arch Clin Exp Ophthalmol* 1999; 237: 654-660.
18. Blasiak A, Blasiak T, Lewandowski MH. Electrophysiology and pharmacology of the optic input to the rat intergeniculate leaflet *in vitro*. *J Physiol Pharmacol* 2009; 60: 171-180.
19. Jernajczyk W, Sobanska A, Czerwosz L, Szatkowska E. The influence of age and gender on the latency of eye movement in healthy humans. *J Physiol Pharmacol* 2005; 56(Suppl. 4): 93-97.

Received: December 19, 2012

Accepted: June 10, 2013

Author's address: Zisis Gatzios, Department of Ophthalmology, University Hospitals of Geneva HUG, 22 Rue Alcide-Jentzer, 1211 Geneva, Switzerland.

E-mail: zisisg@hotmail.com